Analytical Sciences
Advance Publication by J-STAGE
Received June 27, 2020; Accepted August 17, 2020;
Published online on August 28, 2020
DOI: 10.2116/analsci.20P228

Fluorescent and colorimetric dual-signal enantiomers recognition via enzyme catalysis: The case of glucose enantiomers using nitrogen-doped silicon quantum dots/silver probe coupled with β-D-glucose oxidase

Yinhui Yi* [a,b], Lirong Liu[a], Yuntao Wu[a], Gangbing Zhu[a,b]

[a] School of the Environment and Safety Engineering, Jiangsu University, Zhenjiang, 212013, P. R. China

[b] State Key Lab oratory of Chemo/Biosensing and Chemometrics, Hunan University, Changsha 410082, P. R. China

Abstract

Chiral enantiomers recognition is important but facing tough challenges in the direct quantitative determination for complex samples. In this work, via chosing nitrogen-doped silicon quantum dots (N-SiQD) as optical nanoprobe and constructing N-SiQD/silver (N-SiQD/Ag NPs) complex, β-D-GOx as model enzyme and glucose enantiomers as analytes, a fluorescent and colorimetric dual-signal chiral sensing strategy was proposed herein for chiral recognition based on specific enzyme-catalyzed reaction. N-SiQD can exhibit intense fluorescence, while it can be quenched by Ag NPs owing to the formation of N-SiQD/Ag NPs. In the presence of glucose isomer, D-glucose is catalytically hydrolyzed by β-D-GOx to form H_2O_2 owing to the specific enzyme catalyzed reaction between D-glucose and β-D-GOx, and H_2O_2 can etch Ag NPs from the N-SiQD/Ag NPs probe to change the solution color from brown to colorless and restore the N-SiQD fluorescence; while these phenomena cannot be caused by L-glucose, a dual-signal sensing method was thus constructed for recognizing glucose enantiomers. It is believed that the chiral enantiomers recognition strategy via

* Corresponding author. Tel.: +86 511 88791800; fax.: +86 511 88791800.
E-mail address: yyh1108@ujs.edu.cn.

Analytical Sciences
Advance Publication by J-STAGE
Received June 27, 2020; Accepted August 17, 2020;
Published online on August 28, 2020
DOI: 10.2116/analsci.20P228

enzyme catalysis has great application for selective and quantificationally detection of enantiomers in the complex sample system.

Keywords: Chiral recognition; Chiral sensing; enantiomers; silicon quantum dots; fluorescence sensing.

Introduction

Chirality has a significant influence toward chem/biological research because most of the active substances hold chirality. In general, the toxicity, biochemical activity and metabolic pathways of chiral enantiomers are very different. Whereas one isomer has little desirable value or even causes though side-effect, the other can exhibits perfect activity.[1-3] Therefore, considering the practical importance of chiral enantiomers, the development of effective techniques for chiral sensing is of great significance in various fields.[4,5] Due to the advantageous features in cost, simplicity, sensitivity, real-time analysis and automation, optical techniques have attached substantial interests from researchers in recent years.[6-8] On the basic of the structural features and constitutional components, the developed chiral sensing can be divided to metal complex based- and polymer based-chiral probes, organic small molecule based- and nanomaterial based-chiral sensors.[9-11] For instance, Noguchi et al.[12] designed oligophenylenevinylene-based fluorescent chiral sensor for 1,2-cyclohexanedicarboxylic acid enantiomers; Wen et al.[13] synthesized a fluorescent molecular probe (1,1′-bi-2-naphthol-based bis(naphthylimine) compound (R)-4) for detecting chiral functional amines.

No question that the previous studies for chiral sensing are very important and accelerate greatly the development of analytical-technological for enantiomers recognition, but almost of all the works only can detect the ratio of chiral isomers in the racemic mixture, but they cannot obtain the directly quantitative and selective detection.[14,15] In addition, these chiral sensing platform generally involve only single signal mechanism, which would be not believable enough owing to the interfere (e.g. testing surroundings&mistakes). While the sensors with multiple signallings can enable testing

Analytical Sciences
Advance Publication by J-STAGE
Received June 27, 2020; Accepted August 17, 2020;
Published online on August 28, 2020
DOI: 10.2116/analsci.20P228

results to be more persuasive, and it's dedicated to offer accessional associated information as well as increase the sensitivity and selectivity.[16-18] In 2019, our group[19] designed an electrochemical chiral recognition method via competitive supramolecular host-guest interactions, which could recognize directly one isomer from racemic mixture, but it still cannot be applied for complex samples. In consequence, developing a multiple signals approach for the quantitative determination of chiral enantiomers in the complex system is undoubtedly very important.

As is well-known, biological enzymes generally show the advantages of high specificity and efficacy, and enzyme-based chem/biosensors have attracted many attentions in various fields.[20-25] Interestingly, many enzymes are natural chiral ligands which could selectively catalyze one isomer reaction while have no capability for the others.[26,27] For instance, many D-amino-acid oxidase and β-D-glucose oxidase (β-D-GOx) could catalyze the corresponding D-isomer to produce H_2O_2 with O_2 consumption, but it has little catalytic performance toward L-isomer. In addition, enzymes generally could be used in complex sample.[28-30] These unique properties of enzyme make it good candidate for constructing chiral recognization platform with excellent applicability and selectivity. On the other hand, the requirements for chiral sensing are not only the recognization of every enantiomer but also suitable nanomaterials enhancing the related responsive signaling. The alliance of enantio-selectivity with optical performances could endowf the conjugated nanohybrids with many significative superiorities as the sensing elements.[31-35] As a novel abundant and low-cost fluorescent nanomaterial, the eco-friendly silicon quantum dots (SiQD) have attracted much attention as fluorescent probes, [36-39] and SiQD are much more superior in photostability, water solubility, photoluminescence profiles and cytotoxicity comparing to the other semiconductor quantum dots.[40-43] The interesting advantages of SiQD enable them to be a perfect candidate to construct multiple signaling sensor for chiral recognizing.

Most recently, many H_2O_2 etching-based sensors have been proposed,[44-46] inspired by this and above insights, in this work, firstly the nitrogen doping SiQD (N-SiQD) and N-SiQD/silver nanoparticles complex (N-SiQD/Ag NPs) were synthesized (Scheme S1), in which the fluorescence

Analytical Sciences
Advance Publication by J-STAGE
Received June 27, 2020; Accepted August 17, 2020;
Published online on August 28, 2020
DOI: 10.2116/analsci.20P228

quenching of N-SiQD originates from Ag NPs owing to their closeness; then, through choosing β-D-GOx as model enzyme and D-/L-glucose (typical chiral molecules; due to their different preoperties, their effective identification is highly critical[47,48]) as analytes, a fluorescent and colorimetric dual signals sensing platform based on enzyme catalysis reaction were proposed herein for the first time in chiral sensing (Scheme 1). For D-glucose, β-D-GOx can catalyze it to produce H_2O_2 to etch Ag NPs, which further results in the release of N-SiQD from the N-SiQD/Ag NPs complex coupled with the increasement of corresponding fluorescence intensity and the color change from brownish yellow to colorless. As for L-glucose, it cannot be catalyzed by β-D-GOx. Based on the above principle, the straightforward and selective determination of D-glucose was achieved with fluorescent and colorimetric double signals; more interestingly, the enantiomers sensing platform for D-glucose proposed herein can be applicable for the complex system. What is certain is that the presented chiral enantiomers sensing strategy with double signaling via specific enzyme-catalyzed reaction offers an universal approach for chiral enantiomers in the complex system, which would play a highly significant role in the field of chiral sensing and have important application values.

Experiment section

Preparing N-SiQD and N-SiQD/Ag NPs

The preparation processes of N-SiQD and N-SiQD/Ag NPs were similar with our previous work.[49] in brief, 5.4 mg of o-phenylenediamine (OPD) was added firstly to 5.0 mL 20% (v/v) 3-[2-(2-aminoethylamino)ethylamino]propyl-trimethoxysilane (NAE) solution under stirring, and consecutively the mixture was transferred into the autoclave with teflon lined for 4 h at 200 ℃. In the end, by cooling and purification with a dialysis tube for ~6 h, N-SiQD were obtained successfully and stored at 4 ℃ for further use. For preapring N-SiQD/Ag NPs, 1.0 mL $AgNO_3$ was added into the 2.0 mL N-SiQD solution to present a final concentration of 10-fold diluted N-SiQD; then, 1.0 mL fresh $NaBH_4$ (4.0 mM) solution was added, and shake vigorously for 10 min

Analytical Sciences
Advance Publication by J-STAGE
Received June 27, 2020; Accepted August 17, 2020;
Published online on August 28, 2020
DOI: 10.2116/analsci.20P228

subsequently. The change of the mixed solution from yellow to brown indicates the formation of N-SiQD/Ag NPs.

Chiral determination

The chiral sensing for glucose enantiomers was carried out according to the following sprocedures: a 250 μL of glucose isomer samples at various concentrations were incubated with β-D-GOx (50 μg/mL) in Tris buffer (pH 7.4, 10 mM) for 30 min at 37.0 ℃, and 250 μL of N-SiQD/Ag NPs was introduced into the above reaction mixture subsequently. The fluorescence and absorbance spectrums were recorded after 10 min.

Analysis of Real Sample

The human serums samples were obtained from Jiangsu University Hospital. Before analysis, the serum samples were centrifuged at 10000 rpm for 10 min to collect supernatant serums for further measurement. The standard addition method was employed to check the suitability of the sensor. 0, 0.5 and 5.0 mM D-glucose was added to the human serums, and the total volume of the reaction system is 500 μL. Firstly, a 250 μL of Tris buffer containing 10 μL of serum and β-D-GOx (50 μg/mL) , follow by incubation at 37 ℃ for 30 min . Secondly, 250 μL N-SiQD/Ag NPs was added to the reaction mixture, and the fluorescence and absorption spectra of resultant solutions were recorded after the incubation of 10 min.

Result and discussion

Characterization of N-SiQD

The transmission electron microscopy (TEM) images and size distributions of the produced N-SiQD and N-SiQD/Ag NPs were shown in Figure 1. It's noted from Figure 1a that N-SiQD are uniform and the average diameter is ~4.0 nm. As for N-SiQD/Ag NPs (Figure 1b), N-SiQD combines well with Ag NPs and the diameter of N-SiQD/Ag NPs is increased to ~15.0 nm, and the content of Ag in N-SiQD/Ag NPs was obtained to be 32.62 wt% through inductively coupled plasma-atomic emission spectroscopy. In addition, the Energy Dispersive X-ray spectroscopy (EDS) pattern from N-SiQD indicates that C, N, Si and O elements are presented in N-SiQD

Analytical Sciences
Advance Publication by J-STAGE
Received June 27, 2020; Accepted August 17, 2020;
Published online on August 28, 2020
DOI: 10.2116/analsci.20P228

(Figure 2a), and the X-ray diffraction (XRD) analysis shows a typical broad diffraction peaks in the range of 15–25 degrees and strong Si peak at (111) plane at ~27.2 ° (Figure 2b), indicating that N-SiQD are in the amorphous phase.[50,51] As for the typical FT-IR analysis of the as-prepared N-SiQD (Figure 2c), the peak at 3354 cm^{-1} could be ascribed to the N-H stretching vibrations, and the fairly strong absorption peak at 2933 cm^{-1} can be attributed to O-H bending vibration. Meanwhile, the absorption band appears at 1566 cm^{-1} indicated the existence of N-H. The above results suggested that N-SiQD prossess abundant amino and hydroxyl groups that can greatly improve the stability and solubility of N-SiQD.

Quenching mechanism investigation

The working principle of this dual signal sensor was illustrated in Scheme 1. Firstly, the added Ag^+ can interact with the surface of the N-SiQD through the carboxyl, amino and other functional groups. Then, N-SiQD/Ag NPs nanocomplexes were formed by the use of $NaBH_4$ to reduce a mixture of Ag^+ and N-SiQD. As a consequence, the Ag NP can effectively quench the fluorescence of N-SiQD due to FRET. The optical properties of N-SiQD and N-SiQD/Ag NPs were studied to prove the quenching mechanism. It can be seen in Fig. 3 that the absorption spectrum of N-SiQD/Ag NPs (centered at 410 nm) and the emission spectrum of N-SiQD (centered at 450 nm) have a large overlap. This is a necessary condition for FRET.[52] Thus, FRET from SiQDs to AgNPs can be described as the mechanism of AgNPs quenching SiQDs. When H_2O_2 produced by the enzymatic reactions between D-glucose and β-D-Gox existed in the solution, it can etch Ag NPs to form silver ions, thereby releasing N-SiQD and regenerating the fluorescence of N-SiQD. As for L-glucose, the fluorescence was not regenerated since there is no enzymatic reactions between L-glucose and β-D-GOx. Therefore, the fluorescence probe was established and it can be used for the quantitative assay of D-glucose.

Chiral recognition of glucose enantiomers

The feasibility of the developed sensor herein for the recognition of glucose enantiomers was described in detail. As displayed in Figure 3a, the pure N-SiQD can emit strong fluorescence at 450

Analytical Sciences
Advance Publication by J-STAGE
Received June 27, 2020; Accepted August 17, 2020;
Published online on August 28, 2020
DOI: 10.2116/analsci.20P228

nm, but the fluorescence from the prepared N-SiQD/Ag NPs nanocomposites is strongly weak owing to fluorescence quenching of Ag NPs. When D-glucose and β-D-GOx were presented in the N-SiQD/Ag NPs solution, the fluorescence from N-SiQD was regenerated coupled with the strong intensity resulted from the specific enzyme-catalyzed reaction between D-glucose and β-D-GOx. As for L-glucose, the fluorescence was not regenerated since there is no enzymatic reactions between L-glucose and β-D-GOx. Figure 3b showed the absorption spectras of various solution, it's noted that the pure N-SiQD solution cannot show absorption peak, but the N-SiQD/Ag NPs solution exhibits obvious absorption peak at 410 nm owing to the presence of Ag NPs. Similar to the study in fluorescence method, when D-glucose and β-D-GOx, were added to the N-SiQD/Ag NPs solution, the absorbance at 410 nm decreased dramatically because Ag NPs are etched by H_2O_2 which was produced by the enzymatic reactions between D-glucose and β-D-GOx; but for L-glucose, there is no enzymatic reactions between it and β-D-GOx thus the absorbance at 410 nm is reduced little. These results have also been verified by colorimetric observations inset in Figure 3b.

TEM assays were performed to further confirm the chiral recognition mechanism for glucose enantiomers. When D-glucose and β-D-GOx were added to the N-SiQD/Ag NPs solution, the free N-SiQD were presented in TEM images owing to the corrosion of Ag NPs (Figure S1a). While L-glucose and β-D-GOx were present in the solution, there is little change observed from Figure S1b compared to Figure 1b. These results are consistent with the above spectrum and demonstrate also the chiral detection mechanism.

Optimization of conditions

For enhancing the sensitivity of the sensing platform toward glucose, the experimental conditions including the buffer type, the amount of β-D-GOx and reaction time of the enzymatic reaction mediated by β-D-GOx were optimized. As indicated in Figure S2, the highest fluorescence ratio (F/F_0) was obtained in Tris buffer (10.0 mM, pH 7.4). Hence, the final selection of Tris buffer (10 mM, pH 7.4) was the best buffer type for the fluorescence probe. Another crucial factor of the sensing system is the amount of β-D-GOx, thus different β-D-GOx concentrations (25, 50, 100, and

Analytical Sciences
Advance Publication by J-STAGE
Received June 27, 2020; Accepted August 17, 2020;
Published online on August 28, 2020
DOI: 10.2116/analsci.20P228

200 μg/mL) were selected to oxidize D-glucose. As seen from Figure S3, the optimal fluorescence ratio can be obtained by utilizing 50 μg/mL β-D-GOx. The reaction time of β-D-GOx-mediated enzymatic reaction was also investigated for the sake of getting optimum performance, which was conducted at four time points (0, 15, 30, and 45 min). From Figure S4, it's found that 30 min is the best choice for the time. Therefore, the subsequent fluorescent measurements adopts the 30-minute incubation time.

Quantification chiral detection of glucose

Under the optimal experimental conditions mentioned above, the fluorescence and absorbance signal changes of the N-SiQD/Ag NPs probe toward glucose enantiomers at different concentrations were measured. As seen from Figure 4a, the fluorescence intensities of sensing system increase significantly as the increasement of D-glucose concentrations, which confirms that the efficient distinction of glucose enantiomers thanks to the fluorescence quenching of N-SiQD by the decreased amount of Ag NPs. In contrast, the absorption intensity of the sensing system gradually decreases as the enhancement of the D-glucose concentration (Figure 4b). As for L-glucose, there is hardly change in the fluorescence intensities or absorption intensity with the increase of its levels.

Furthermore, we quantify the concentration of D-glucose through the β-D-GOx-mediated reaction system. It was noted from Figure 5a/4b that the fluorescence peak at 450 nm increases gradually after the gradual addition of D-glucose, and there is an excellent plotted linearity between the fluorescence intensity and D-glucose concentration within the range of 1.0 - 200.0 μM with the linear equation of F/F_0-1=0.021[D-glucose]-0.017 (R^2 =0.999), and the limit of detection (LOD) for D-glucose is 0.3 μM (3σ/slope, where σ is the standard deviation of the blank samples). Hence, it can be seen from Figure 5c/4d that the UV–vis absorbance peak around 410 nm decreases with the increasement of D-glucose concentrations from 1.0 to 400.0 μM and shows a good linear relationship in the 1.0 to 200.0 μM range, which was fitted by $1-A/A_0$=0.0035[D-glucose]+0.0033 with the correlation coefficient R^2 of 0.997, and the LOD was calculated to be 0.8 μM (3σ/slope). Conmpard to the previous work for chiral glucose sensor,[53] the proposed method in this work is

Analytical Sciences
Advance Publication by J-STAGE
Received June 27, 2020; Accepted August 17, 2020;
Published online on August 28, 2020
DOI: 10.2116/analsci.20P228

more sensitive and low cost; inaddition, this work introduced new application of SiQD. Insert in Figure 5b and Figure 5d are the digital pictures under UV and visible light of reaction system in the presence of various concentrations of D-glucose, which manifests that D-glucose catalyzed by β-D-GOx to produce H_2O_2 and etching Ag NPs which result in the fluorescence and color change.

Selectivity and application in real samples

The most important innovation of this work is that the developed chiral sensing platform based on specific enzyme-catalyzed reaction can be used in complex samples, thus the selectivity and application in real samples were investigated**.**

First, the selectivity of the proposed D-glucose sensor was evaluated by analyzing multiplex potential interferents, including common substances (L-glucose, sucrose, lactose, galactose, mannose, fructose, xylose) and metal ions (K^+, Ga^{2+}, Na^+, and Mg^{2+}). As shown in Figure 6, most of these interferents have negligible effect on the fluorescence response of 150.0 μM D-glucose even at relatively high concentrations (other interferences were 500.0 μM). Then, the application of N-SiQD/Ag NPs nanocomplex as dual signal probe in human serum samples was studied and the corresponding results were displayed in Table 1. The concentrations of D-glucose were calculated by adopting the calibration equation. The results given in Table 1 demonstrate that the measured recovery rate for samples were over the range of 96.2%-103.9%. These results suggest that the present sensing system is capable of recognizing glucose isomers in complex samples and enable potential practicability in the analysis of real samples for D-glucose.

Conclusion

By designing N-SiQD and N-SiQD/Ag NPs as nanoprobes, β-D-GOx as model enzyme and glucose enantiomers served as analytes, an optical chiral sensor with dual signal based on the specific enzyme-catalyzed reaction was presented for the first time in the optical chirality sensing. Compared with previously reported chiral sensing methods, the developed proposal herein can diametrically quantify and determine chiral enantiomers in the complex system, thus expanding up the application range from the single system (only one species of enantiomer) or racemic mixture

Analytical Sciences
Advance Publication by J-STAGE
Received June 27, 2020; Accepted August 17, 2020;
Published online on August 28, 2020
DOI: 10.2116/analsci.20P228

made to the complex samples. In terms of chiral sensing of glucose enantiomers, by using N-SiQD/Ag NPs as probe, a dual signal sensor platform with low background signal and low detection limit, high sensitivity and excellent selectivity was developed successfully. After distinguishing between glucose isomers, we further quantified D-glucose and tested it in actual serum samples. It is believed that this work possesses significant applications prospect for identifying and detecting glucose enantiomers along with other enantiomers through modifying interrelated substrates and enzymes (e.g. using D-amino-acid oxidase to recognize amino-acid enantiomers via a similar proposal); meanwhile, the strategy proposed through specific enzyme-catalyzed reaction is applicable to chiral identification by other approaches as well, such as electrochemistry, capillary electrophoresis and circular dichroism spectroscopy.

Acknowledgments

We are grateful to the support from the National Natural Science Foundation of China (21607061), the Priority Academic Program Development of Jiangsu Higher Education Institutions, Collaborative Innovation Center of Technology and Material of Water Treatment.

References

1. Z. Lu, X. Lu, Y. Zhong, Y. Hu, G. Li, and R. Zhang, *Anal. Chim. Acta*, **2019**, *1050*, 146.

2. G. Zhu, O. J. Kingsford, Y. Yi, and K.y. Wong, *J. Electrochem. Soc.*, **2019**, *166*, H205.

3. Y. Jiang, C. Liu, X. Wang, T. Wang, and J. Jiang, *Langmuir*, **2017**, *33*, 7239.

4. Z. He, S. Zang, Y. Liu, Y. He, and H. J. B. Lei, *Biosens. Bioelectron.*, **2015**, *73*, 85.

5. D. Wu, Y. Yu, J. Zhang, L. Guo, and Y. Kong, *ACS Appl. Mater.Inter.*, **2018**, *10*, 23362.

6. S. K. Munusamy, K. Thirumoorthy, V. P. Muralidharan, U. Balijapalli, and S. K. Iyer, *Sensors Actuat. B: Chem.*, **2017**, *244*, 175.

7. P. Cai, D. Wu, X. Zhao, and Y. Pan, *Analyst*, **2017**, *142*, 2961.

8. X. Zhang, Q. Yu, S. Chen, and Z. Dai, *New J. Chem.*, **2018**, *42*, 4045.

9. M. Kawai, A. Hoshi, R. Nishiyabu, and Y. Kubo, *Chem. Commun.*, **2017**, *53*, 10144.

Analytical Sciences
Advance Publication by J-STAGE
Received June 27, 2020; Accepted August 17, 2020;
Published online on August 28, 2020
DOI: 10.2116/analsci.20P228

10. X. Zhang, C. Wang, P. Wang, J. Du, G. Zhang, and L. Pu, *Chem. sci.,* **2016**, *7*, 3614.

11. Z.Y. Lin, X.Y. Han, Z.H. Chen, G. Shi, and M. Zhang, *J. Mater. Chem. B*, **2018**, *6*, 6877.

12. T. Noguchi, B. Roy, D. Yoshihara, J. Sakamoto, T. Yamamoto, and S. J. A. C. Shinkai, *Angew. Chem. Int. Edit.,* **2017**, *129*, 12692.

13. K. Wen, S. Yu, Z. Huang, L. Chen, M. Xiao, X. Yu, and L. J. J. o. t. A. C. S. Pu, *J. Am. Chem. Soc.*, **2015**, *137*, 4517.

14. H. Fu, O. Hu, Y. Fan, Y. Hu, J. Huang, Z. Wang, and Y. She, *Sensors Actuat. B: Chem.,* **2019**, *287*, 1.

15. C. Zeng, X. Zhang, and L. Pu, *ACS Omega*, **2018**, *3*, 12545.

16. J. Deng, Q. Lu, Y. Hou, M. Liu, H. Li, Y. Zhang, and S. J. A. c. Yao, *Anal. Chem.*, **2015**, *87*, 2195.

17. H. Ouyang, Q. Lu, W. Wang, Y. Song, X. Tu, C. Zhu, J. N. Smith, D. Du, Z. Fu, and Y. J. A. c. Lin, **2018**, *90*, 5147.

18. B.-C. Iacob, E. Bodoki, A. Florea, A. E. Bodoki, and R. J. A. c. Oprean, *J. Am. Chem. Soc.*, **2015**, *87*, 2755.

19. Y. Yi, D. Zhang, Y. Ma, X. Wu, and G. Zhu, *Anal.Chem.* **2019**, *91*, 2908.

20. C. Zhang, H. Cui, Y. Han, F. Yu, and X. Shi, *Food Chem.,* **2018**, *240*, 893.

21. L. Jiang, D. Wei, K. Zeng, J. Shao, F. Zhu, and D. Du, *Food Anal. Method.*, **2018**, *11*, 2066.

22. W. Li, D. Liu, X. Bi, and T. You, *Sensors Actuat. A-phy.,* **2020**, *302*, 111794.

23. F. Sarpong, P. Otengdarko, M. K. Golly, L. P. Amenorfe, M. T. Rashid, and C. Zhou, *J. Food Biochem.,* **2018**, *42*, e12681.

24. J. Ning, W. Wang, G. Ge, P. Chu, F. Long, Y. Yang, Y. Peng, L. Feng, X. Ma, and T. D. James, *Angew. Chem. Int. Edit.,* **2019**, *58*, 9959.

25. L. Miao, C. Zhu, L. Jiao, H. Li, D. Du, Y. Lin, and Q. Wei, *Anal. chem.,* **2018**, *90*, 1976.

26. R. Ebaid, H. Wang, C. Sha, A. E. Abomohra, and W. Shao, *J. Clean. Prod.*, **2019**, *238*, 117925.

27. L. Wang, W. Li, Y. Liu, W. Zhi, J. Han, Y. Wang, and L. Ni, *Food Chem.,* **2019**, *282*, 48.

Analytical Sciences
Advance Publication by J-STAGE
Received June 27, 2020; Accepted August 17, 2020;
Published online on August 28, 2020
DOI: 10.2116/analsci.20P228

28. G. Carrea, and S. Riva, *Angew. Chem. Int. Edit.*, **2000**, *39*, 22264.

29. A. Haouz, C. Twist, C. Zentz, P. Tauc, and B. Alpert, *Eur. Biophys. J.*, **1998**, *27*, 19.

30. M. S. Reid, X. C. Le, and H. Zhang, *Angew. Chem. Int. Edit.*, **2018**, *57*, 11856.

31. L. Liu, G. Zhu, W. Zeng, B. Lv, and Y. Yi, *Anal. Bioanal.Chem.*, **2019**, *411*, 1561.

32. Y. Yi, L. Liu, W. Zeng, B. Lv, and G. Zhu, *Microchem.Journal*, **2019**, *147*, 245.

33. Y. Yang, B. Mao, G. Gong, D. Li, Y. Liu, W. Cao, L. Xing, J. Zeng, W. Shi, and S. Yuan, *Int. J. Hydrogen Energ.*, **2019**, *44*, 15882.

34. J.W. Zhou, X.M. Zou, S.H. Song, and G.H. Chen, *J. Agr. Food Chem.*, **2018**, *66*, 1307.

35. X. Zhang, X. Yu, J. Wang, Q. Wang, H. Meng, and Z. Wang, *Food Anal.Method.*, **2018**, *11*, 2569.

36. Z. L. Wu, M. X. Gao, T. T. Wang, X. Y. Wan, L. L. Zheng, and C. Z. J. N. Huang, **2014**, *6*, 3868.

37. Z. Tang, Z. Lin, G. Li, and Y. J. A. c. Hu, *Anal. Chem.*, **2017**, *89*, 4238.

38. C. Yang, S. Zhu, Z. Li, Z. Li, C. Chen, L. Sun, W. Tang, R. Liu, Y. Sun, and M. J. C. C. Yu, *Chem. Commun.*, **2016**, *52*, 11912.

39. W.Y. Zhou, S.S. Li, X.Y. Xiao, S.H. Chen, J.H. Liu, and X.J. Huang, *Chem. Commun.*, **2018**, *54*, 9329.

40. Y. Han, Y. Chen, J. Feng, J. Liu, S. Ma, and X. J. A. c. Chen, *Anal. Chem.*, **2017**, *89*, 3001.

41. J. Wu, J. Dai, Y. Shao, and Y. J. R. A. Sun, *RSC Adv.*, **2015**, *5*, 83581.

42. W. Zeng, D. Huang, G. Zhu, B. Lv, and Y. Yi, *Anal. Sci.*, **2020**, 10.2116/analsci.20p011.

43. L. Liu, G. Zhu, W. Zeng, Y. Yi, B. Lv, J. Qian, and D. Zhang, *Microchim. Acta*, **2019**, *186*, 98.

44. Y. Xia, J. Ye, K. Tan, J. Wang, and G. Yang, *Anal.Chem.*, **2013**, *85*, 6241.

45. X. Yang, Y. Yu, and Z. Gao, *ACS Nano*, **2014**, *8*, 4902.

46. L. Huang, C. Yuan, W. Chen, F. Zeng, H. Xu, Y. Zhang, and T. Jiang, *Nano*, **2018**, *13*, 1850022.

47. C.S. Zhang, S. A. Hawley, Y. Zong, M. Li, Z. Wang, A. Gray, T. Ma, J. Cui, J.W. Feng, M. Zhu, Y.Q. Wu, T. Y. Li, Z. Ye, S.Y. Lin, H. Yin, H.L. Piao, D. G. Hardie, and S.C. Lin, *Nature*, **2017**, *548*, 112.

Analytical Sciences
Advance Publication by J-STAGE
Received June 27, 2020; Accepted August 17, 2020;
Published online on August 28, 2020
DOI: 10.2116/analsci.20P228

48. Y. Sun, Y. Mei, J. Quan, X. Xiao, L. Zhang, D. Tian, and H. Li, *Chem. Commun.*, **2016**, *52*, 14416.

49. G. Zhu, D. Huang, L. Liu, Y. Yi, Y. Wu, and Y. Huang, *Anal. Lett.*, **2020**, 10.1080/00032719.2020.1720222.

50. A. Samavati, Z. Othaman, S. Dabagh, and S. K. Ghoshal, *J. Nanosci. Nanotechno.*, **2014**, *14*, 5266.

51. S. Shen, B. Huang, X. Guo, and H. Wang, *J. Mater. Chem. B*, **2019**, *7*, 7033.

52. X. Bi, L. Luo, L. Li, X. Liu, B. Chen, and T. You, *Talanta*, **2020**, *218*, 121159.

53. J. Zhou, J. Duan, X. Zhang, Q. Wang, and D. Men, *Nanoscale*, **2018**, *10*, 18606.

Analytical Sciences
Advance Publication by J-STAGE
Received June 27, 2020; Accepted August 17, 2020;
Published online on August 28, 2020
DOI: 10.2116/analsci.20P228

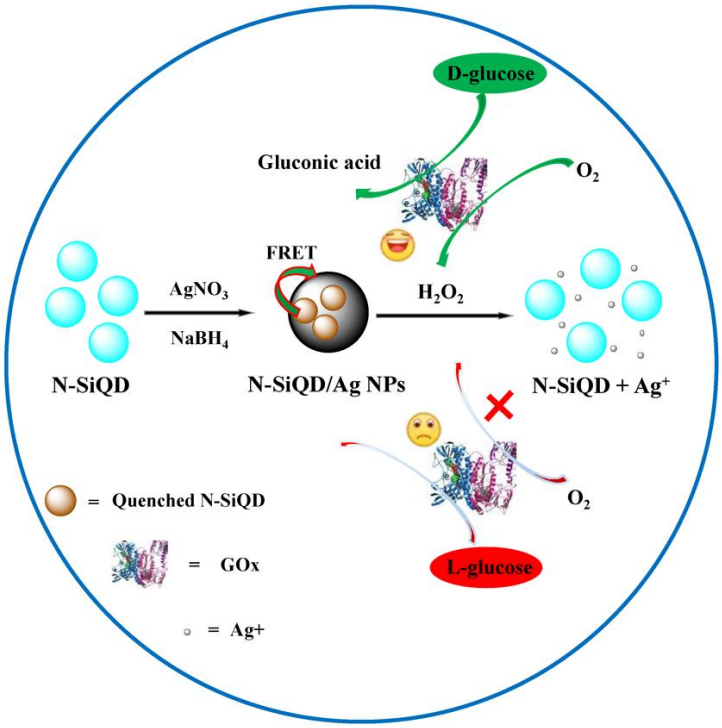

Scheme 1. Schematic illustrations for fluorescent and colorimetric dual-signal chiral recognition of glucose enantiomers based on specific enzyme-catalyzed reaction using N-SiQD/Ag NPs probe coupled with β-D-GOx.

Analytical Sciences
Advance Publication by J-STAGE
Received June 27, 2020; Accepted August 17, 2020;
Published online on August 28, 2020
DOI: 10.2116/analsci.20P228

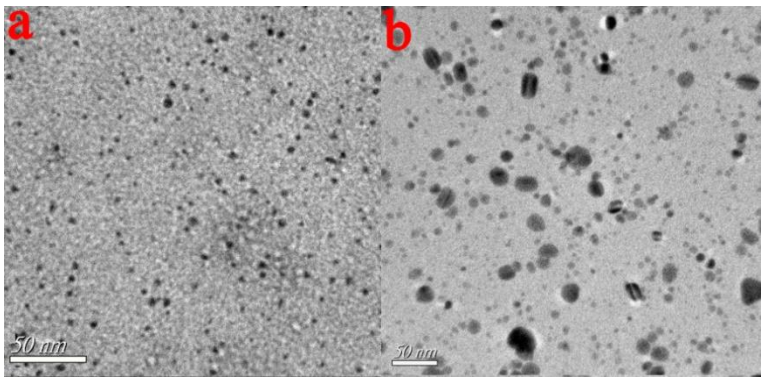

Figure 1. TEM images of SiQD (a) and SiQD/Ag NPs (b)

Analytical Sciences
Advance Publication by J-STAGE
Received June 27, 2020; Accepted August 17, 2020;
Published online on August 28, 2020
DOI: 10.2116/analsci.20P228

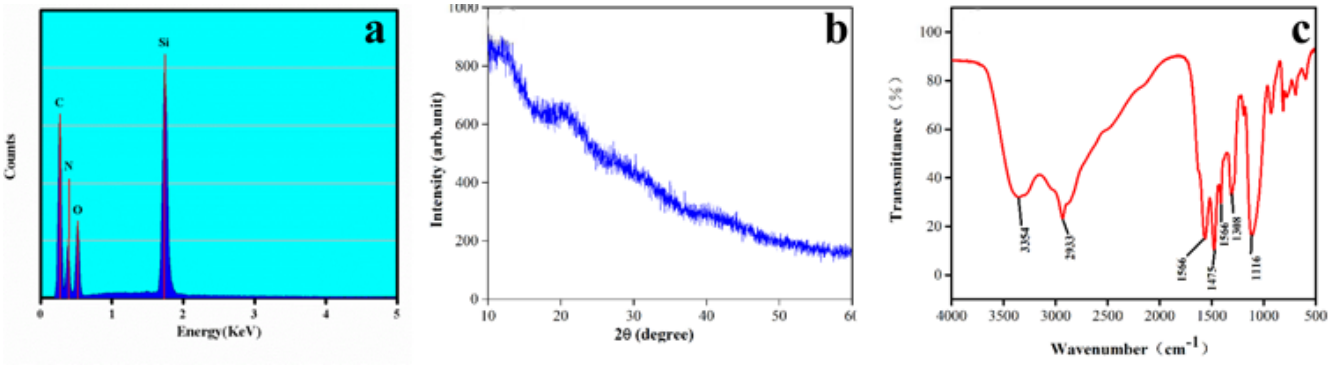

Figure 2. (a) EDS pattern, (b) XRD spectrum, and (c) FT-IR spectrum of the N-SiQD.

Analytical Sciences
Advance Publication by J-STAGE
Received June 27, 2020; Accepted August 17, 2020;
Published online on August 28, 2020
DOI: 10.2116/analsci.20P228

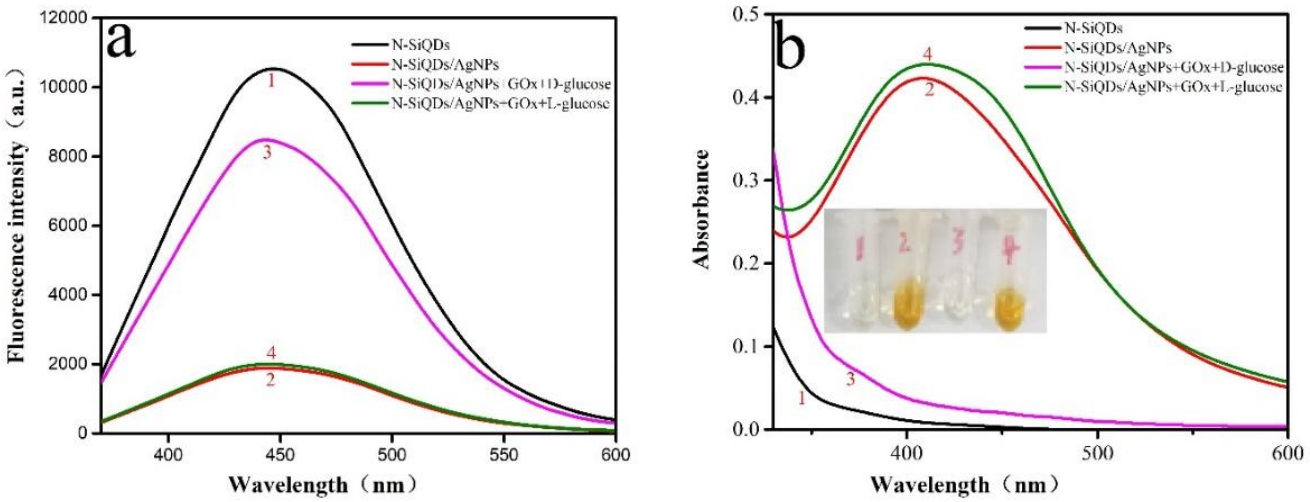

Figure 3. (a) Emission spectra of N-SiQD (black), N-SiQD/Ag NPs (red), β-D-GOx and D-glucose (pink), β-D-GOx and L-glucose (green). (b) Absorption spectra of N-SiQD (black), N-SiQD/Ag NPs (red) and N-SiQD/Ag NPs after adding β-D-GOx and D-glucose (pink), β-D-GOx and L-glucose (green). Insert in (b) shows the photograph of these solutions under visible light. The glucose concentration, 500.0 μM.

Analytical Sciences
Advance Publication by J-STAGE
Received June 27, 2020; Accepted August 17, 2020;
Published online on August 28, 2020
DOI: 10.2116/analsci.20P228

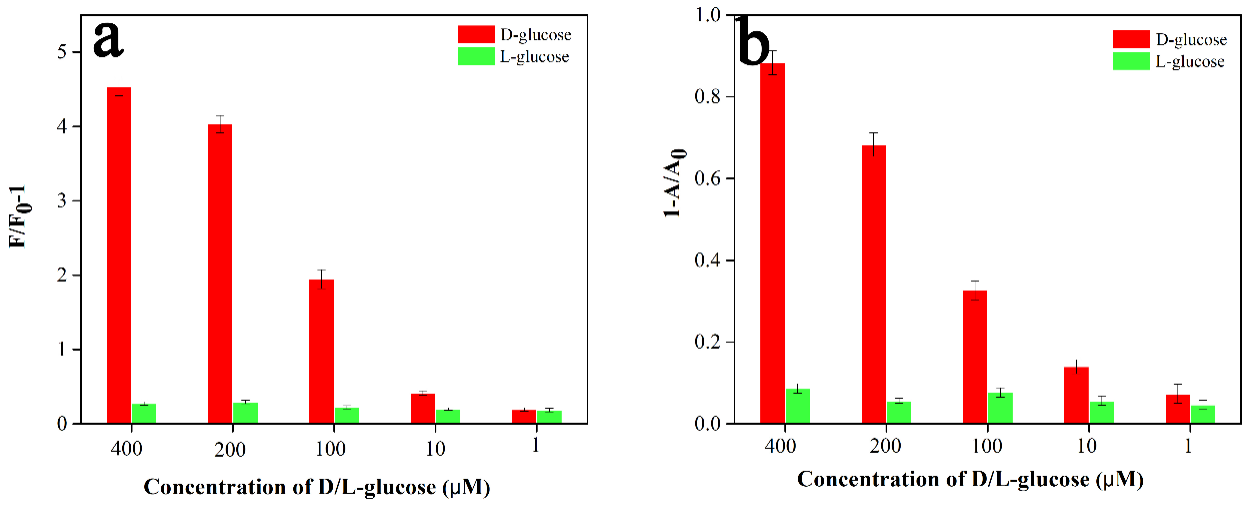

Figure 4. (a) Relative fluorescence variation histogram at different concentrations of D-glucose and L-glucose. (g) Relative UV-Vis absorption variation histogram at different concentrations of D-glucose and L-glucose.

Analytical Sciences
Advance Publication by J-STAGE
Received June 27, 2020; Accepted August 17, 2020;
Published online on August 28, 2020
DOI: 10.2116/analsci.20P228

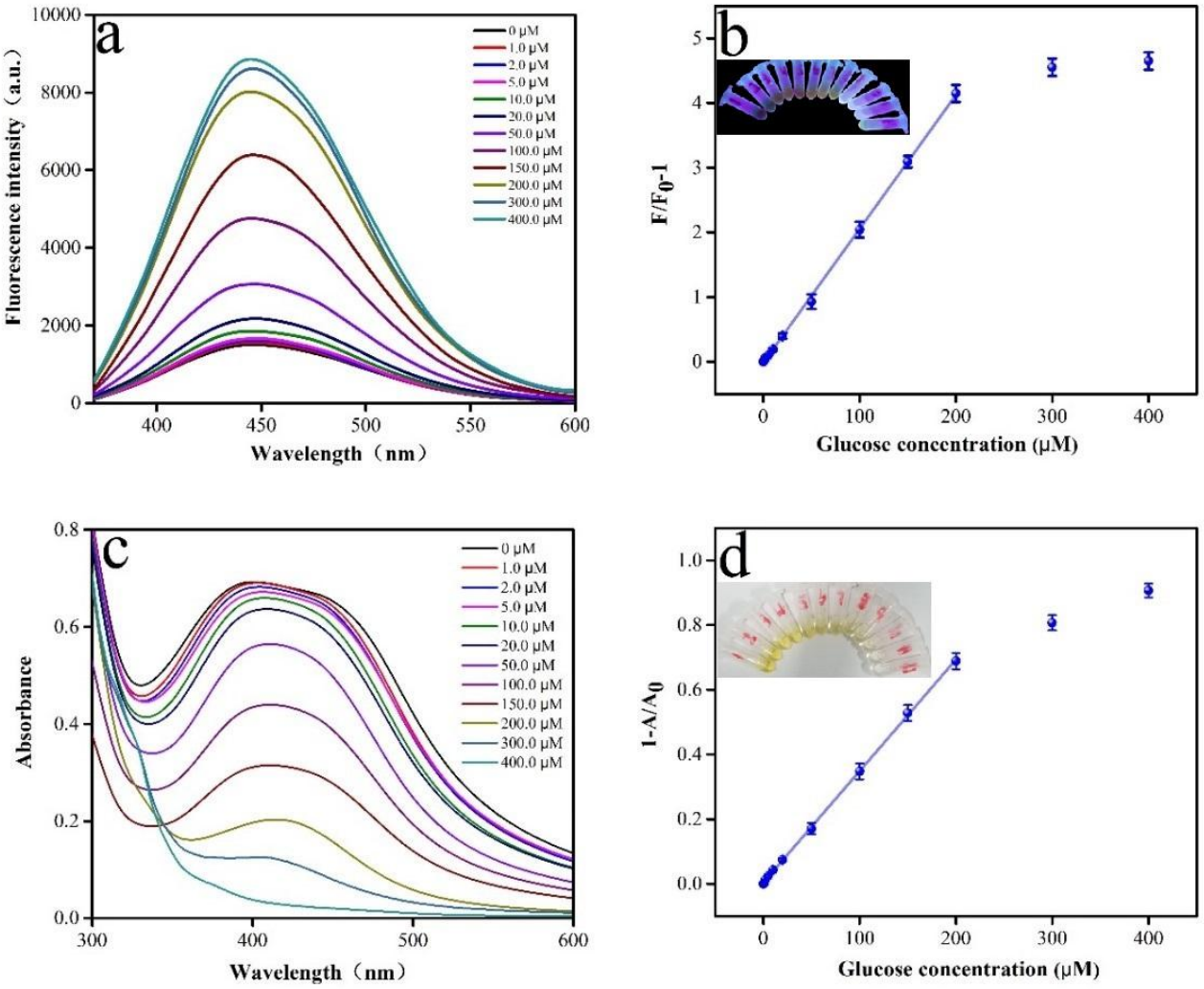

Figure 5. (a) The relationship between the fluorescence intensity of N-SiQD/Ag NPs and the concentration of D-glucose; (b) the calibration curves for the detection of D-glucose. Insert in (b) shows the digital images of change in color of N-SiQD/Ag NPs with addition to different concentrations of D-glucose under UV light (365 nm). (c) the relationship between the absorbance of N-SiQD/Ag NPs and the concentration of D-glucose; (d) the calibration curves for the detection of D-glucose. Insert in (d) shows the digital images of change in color of N-SiQD/Ag NPs with addition to different concentrations of D-glucose under visible light.

Analytical Sciences
Advance Publication by J-STAGE
Received June 27, 2020; Accepted August 17, 2020;
Published online on August 28, 2020
DOI: 10.2116/analsci.20P228

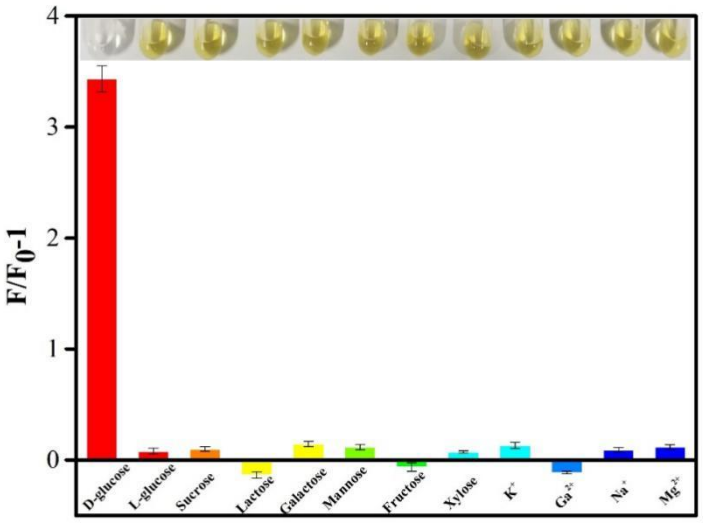

Figure 6. Selectivity analysis for D-glucose detection by the recoveried fluorescence intensities of SiQD/Ag NPs. Insert in this figure shows the digital images of change in color of N-SiQD/Ag NPs with different interferences.

Analytical Sciences
Advance Publication by J-STAGE
Received June 27, 2020; Accepted August 17, 2020;
Published online on August 28, 2020
DOI: 10.2116/analsci.20P228

Table 1. Analysis of D-glucose in serum samples.

Sample	Added (mM)	Found (mM)		Recovery (%)		RSD (%)	
		Fluorimetry	Colorimetry	Fluorimetry	Colorimetry	Fluorimetry	Colorimetry
	0	4.5±0.03	4.6±0.06	——	——	4.26	3.26
	0.5	5.1±0.02	5.3±0.01	102.0	103.9	3.52	4.18
Sample 1	5.0	9.3±0.06	9.8±0.04	97.8	102.1	2.67	3.16
	0	4.8±0.02	4.9±0.5	——	——	3.01	4.25
	0.5	5.5±0.02	5.6±0.02	103.8	103.7	6.72	3.21
Sample 2	5.0	9.6±0.02	9.7±0.02	97.9	98.0	4.11	2.34
	0	4.9±0.05	4.8±0.06	——	——	2.72	3.61
	0.5	5.2±0.02	5.1±0.02	96.3	96.2	2.61	3.34
Sample 3	5.0	10.3±0.02	9.7±0.02	104.0	98.9	2.81	4.42

Analytical Sciences
Advance Publication by J-STAGE
Received June 27, 2020; Accepted August 17, 2020;
Published online on August 28, 2020
DOI: 10.2116/analsci.20P228

Graphical abstract